A novel concept for a reinforced glass beam carrying long term loads

Jens H. Nielsen · Bjarni G. Jónsson · Chiara Bedon

Accepted: 21 August 2020

Abstract This paper presents a novel concept for improving the long-term load-bearing performance of reinforced glass beams (hybrid beams). The concept of reinforcing glass beams using steel or other (ductile) materials have been investigated over the last couple of decades utilising the fracture pattern of annealed glass to ensure a ductile behaviour. However, it is well known that the long-term strength of annealed glass is rather low due to so-called static fatigue leading to a relatively poor performance for most hybrid-beams. As an example will a hybrid beam based on annealed glass exposed to 26 MPa permanent load fail in less than a day according to a European code. The novel concept suggested here utilises a combination of annealed and fully tempered glass in an arrangement where the tempered glass carries the long-term loading whereas short-term loading is carried by the reinforced annealed glass. The concept is based on the relaxation of shear stresses in the PVB (polyvinyl butyral) interlayer, material properties of PVB from different authors have been compared, and a set of average parameters have been suggested. The main purpose of the paper is to introduce the concepts and mechanisms of such beams and provide a basis for further optimisation.

Keywords Hybrid glass beams · PVB interlayer properties · Long term loading · Static fatigue · Tempered glass

J. H. Nielsen (✉)
Departmentt of Civil Engineering, Technical University of Denmark, Brovej Building 118, Lyngby, Denmark
e-mail: jhn@byg.dtu.dk

B. G. Jónsson
EFLA, Reykjavík, Iceland

C. Bedon
University of Trieste, Trieste, Italy

1 Introduction

The use of glass as a load-bearing building component has gained an increasing interest over the last couple of decades. One of the major challenges in the design of glass structures is the brittleness and unfavourable mechanism of failure. Load-carrying composite structural elements of e.g. Timber/glass and concrete/glass have been suggested in the literature (e.g. Ber et al. 2016; Freytag 2004; Vallee et al. 2016). However, most work have been published for Glass/steel composites which have shown that a ductile, safe mechanism of failure can be achieved by bonding steel to the glass analogously to reinforced concrete (Bos et al. 2004; Louter 2011; Nielsen and Olesen 2007, 2010; Ølgaard et al. 2009; Veer et al. 2003; Wellershoff and Sedlacek 2003). This concept has been intensively investigated over the last two decades and papers discussing the use, possible designs and mechanisms

can be found in the literature, see e.g. Bedon and Louter (2016), Cupać et al. (2017), Martens et al. (2016a, b), Martens et al. (2018). The ductility in the existing concept is relying on the fracture of annealed-glass into relatively large pieces capable of keeping the compression zone of the beam usable. However, using only annealed-glass has a major drawback, namely the decay in tensile strength known as static fatigue as described by e.g. Brown (1969), Charles (1958a, b) and incorporated standards such as EN 16612:2019. Assuming a stress of 26 MPa originating from a permanent load on a beam consisting of annealed glass will, according to EN 16612:2019, have a life time of approximately 9 h as will be shown later in this paper (see e.g. Figure 11). This poses a problem since the beam needs to be designed for a significantly reduced tensile strength in case of long-term loading.

The tensile strength of tempered glass is governed by the residual stresses, which are not subjected to any decay over time. However, fracture of tempered glass is still brittle, and furthermore, it fails in small fragments due to the high strain-energy introduced by the residual stresses, see e.g. Nielsen (2017), Nielsen et al. (2009), Nielsen and Bjarrum (2017), Pour-Moghaddam (2020). Obtaining a similar degree of ductility by reinforcing a fully tempered glass compared to an annealed glass beam is not possible. This is due to the fragmentation of the glass and such beams typically fail by local instability of the compression zone in the glass beam, see e.g. Louter et al. (2012). A combination of tempered glass and annealed glass laminated together improves the result, but does not provide the same degree of ductility (Møller and Andersen 2010) and still applies long-term loading to the annealed glass.

The suggested concept consists of laminated annealed- and tempered glass utilising the viscous properties of the laminate to redistribute the long-term loads to the tempered glass. The concept is illustrated in Fig. 1 where it is seen that the load is only introduced in the tempered glass and then transferred, by shear in the laminate, to the annealed glass. The reinforcement is bonded adhesively to the annealed glass alone, not transferring load between tempered- and annealed glass. All load-transfer between tempered and annealed glass will therefore take place through the viscous (PVB) interlayer. This indicates that the shear stresses in the (viscous) interlayer will reduce over time (relaxation) and only (if any) a minor part of the long-term load will be carried by the annealed glass.

However, in case of sudden change in load such as wind gusts or even fracture of the beam, the viscous interlayer will be transferring shear stresses again and the beam will work with combined action to resist the short term load and in case of fracture, activate the reinforcement through the annealed glass. This is illustrated in Fig. 2 where it is seen that the annealed glass part of the beam over time (of constant load) moves towards the initial position, leaving the tempered glass carrying the long-term loads alone.

The present paper considers some preliminary experimental and numerical investigations into the possibilities for creating such beams. The scope of the paper is to justify a plausible concept, not providing an optimal beam design for a specific given condition.

2 Design of a concept beam

According to Nielsen and Olesen (2010), Ølgaard et al. (2009) a reinforced glass beam can be assumed to have four principal failure modes: Anchorage failure, Under-reinforced failure, Over-reinforced failure and Normal-reinforced failure. Anchorage failure is usually due to bonding failure in the glass/steel interface and is a rather common type of failure, which typically occurs when the yield strength of the reinforcement is too high. In that case, the shear stresses transferred by the adhesive become too large and bonding failure occurs before yielding of the reinforcement. An under-reinforced beam fails due to lack of reinforcement strength and in an over-reinforced beam, failure occurs in the compressive zone. A normal-reinforced beam is the preferred behaviour of the beam where the reinforcement yields after glass fracture without adhesive failure setting an upper limit for the yield stress of the reinforcement, thus providing a safe ductile design.

These principles are still valid for the proposed beam design considering the so-called post-fracture limit state as currently discussed for the new eurocode on structural glass, see Feldmann and Di Biase (2018). In the post-fracture limit state, the tempered glass should be neglected in the design due to fragmentation and only the pure annealed glass beam with reinforcement is active. However, in the serviceability limit

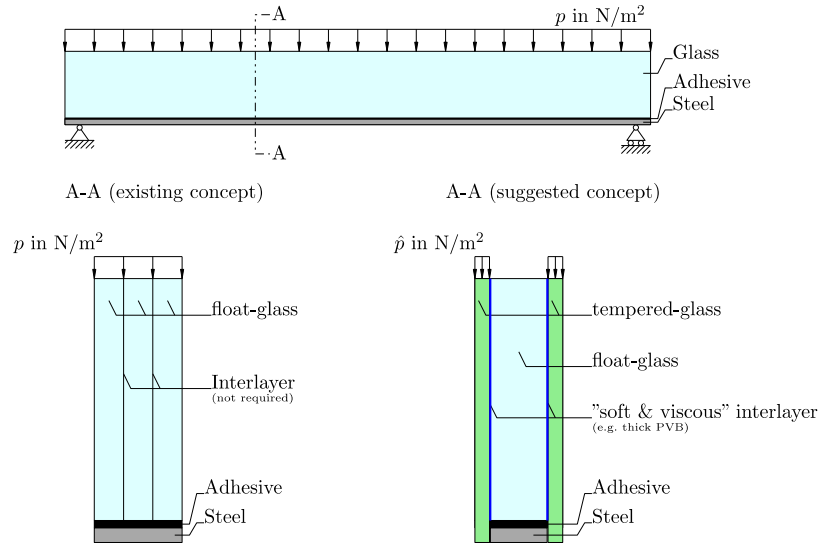

Fig. 1 Existing concept (bottom left), suggested concept (bottom right)

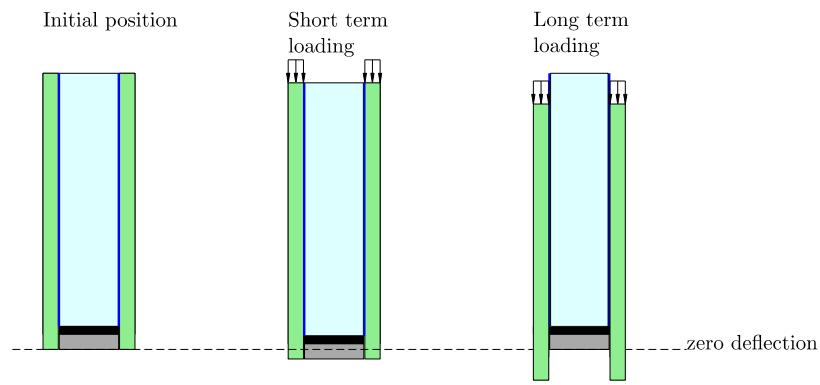

Fig. 2 Principal behaviour of a beam cross-section of the proposed concept. Note that the reinforcement is only adhesively bonded to the annealed glass

state, long term loading is carried by the tempered glass.

The above described failure modes should be accounted for in the post-fracture limit state. For the proposed concept, this indicates that disregarding the tempered glass, the beam should be designed as a reinforced annealed glass beam. This can be done by the method provided in e.g. Nielsen and Olesen (2010). Assuming the tempered glass to carry a load similar to the reinforced annealed glass beam, two plies of 4 mm tempered glass were used in the design as shown in Fig. 3.

These plies of tempered glass were laminated with a thick PVB layer (nominal thickness of 8×0.38 mm = 3.04 mm) to the sides of the annealed glass and the reinforcement was afterwards adhesively bonded to the annealed glass alone using a two component epoxy (DELO-DUOPOX® AD840) with an intended thickness of 0.5 mm.

3 Experimental test of concept beams

The design concept was investigated experimentally using a load-controlled (dead weight) four-point bending test. Six 1000 mm long glass beams were tested, one reference beam without steel reinforcement and five with steel reinforcement. The dimensions, as described in Fig. 3, for the glass beams are given in Table 1 where CBα is the abbreviation for Composite Beam number "α". Furthermore, the applied load, F, along with the dimensions of the statically system, L_b and L_e as shown in Fig. 7 is provided in the table along with the strain measured initially, ϵ_{start}, and after, ϵ_{end} in the annealed glass and the loading time (*Time*). The

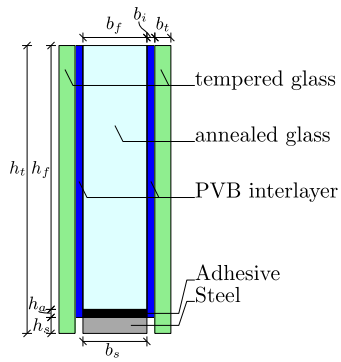

Fig. 3 Experimental design of the glass beam (length of beam, L = 1000 mm)

Dimensions:

b_f, is the thickness of the annealed (float) glass,
b_i, is the thickness of the PVB interlayer,
b_t, is the thickness of the tempered glass,
b_s, is the width of the steel,
h_t, is the height of the tempered glass,
h_f, is the height of the annealed (float) glass,
h_a, is the height of the adhesive layer,
h_s, is the height of the steel

Table 1 Parameters for the experimental tests. CB1 is a first pilot test and is excluded in the results. In CB2 troubles with the gluing was experienced and reliable measurements of h_a is not available. CB5 was tested without reinforcement, but otherwise similar to the other beams

	CB1	CB2	CB3	CB4	CB5	CB6
b_f [mm][a]	18.55	18.62	18.58	18.56	≈18.6	18.62
b_i [mm][b]	2.3	3.1	2.3	2.42	≈2.15	1.2
b_t [mm][a]	3.88	3.78	3.72	3.86	≈3.8	3.85
b_s [mm]	18.58	18.56	18.35	18.48	N/A	18.68
h_t [mm]	90	90	90	90	90	90
h_f [mm]	84	84	84	84	84	84
h_a [mm][c]	0.51	–	0.61	0.52	N/A	0.59
h_s [mm][d]	6.3	5.41	5.44	6.23	N/A	6.24
δ_t [mm][e]	3.2	3.2	3.2	3.2	3.2	3.2
F [kN][f]	2.25/4.71	4.71/5.69	5.69	5.69	5.69	5.69
L_b [mm]	200	200	300	200	300	200
L_e [mm]	40	40	40	40	40	40
$\epsilon_{start} \times 10^{-4}$	–	− 2.86	− 3.26	− 3.61	− 4.1	− 3.63
$\epsilon_{end} \times 10^{-4}$	–	− 1.35	− 1.97	− 2.05	− 1.87	− 2.8
Time (h)	192.25	192.64	190.2	260.7	190.57	163.5
Temp (°C)	–	27 to 35	27 to 34	30 to 36	≈31	28 to 36
Notes	Pilot test (not shown in results)	Troubles with gluing.			Reference, no reinforcement.	

[a]The beams were delivered as laminated and the thickness of the individual glass plies could not be measured everywhere

[b]The thickness of the interlayer (PVB) was found by measuring the total thickness of the beam at the middle (lengthwise), subtracting the glass plies and divide by the two interlayers. Variation of this is found along the beam length due to thinning of the PVB close to the ends

[c]Thickness of the adhesive layer was found by subtracting the height of the annealed glass and the steel from the total beam height

[d]Variations in height of steel is due to grinding and sandblasting to fit the parts

[e]Allowable displacement of the tempered glass relative to the annealed glass due to the loading aggregate as sketched in Fig. 4

[f]The notation 4.71/5.69 indicates a change in load from 4.71 to 5.69 kN to accelerate the tests. For test CB2 the load was increased after 144 h. For the pilot (CB1) the load was increased stepwise (2.25 to 3.75 to 4.71) over more than a week to find the load level

temperature in the experiment was elevated to speed up the tests, however, relatively large fluctuations were observed and *Temp* in the table provides the max. and min. temperatures observed.

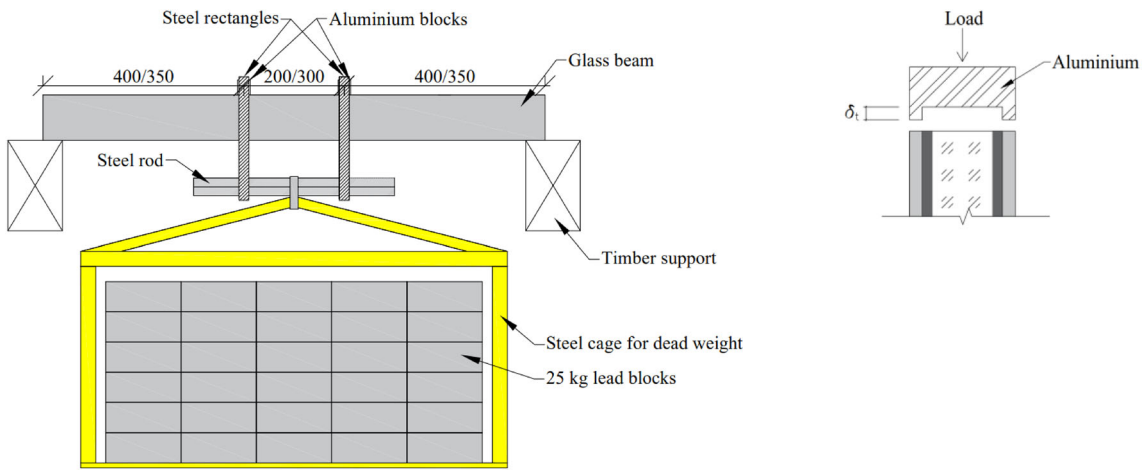

Fig. 4 Set-up of the long-term test. Left: sketch of setup, Right: aluminium blocks for adding loads only on the tempered glass

The long-term experiment on CB1 did not go as planned, which is why only limited useful results could be drawn from that experiment. This was mainly due to how the steel reinforcement was adhesively bonded to the annealed glass, and how the support conditions were applied.

The test set-up for the long-term loading experiment is shown in Fig. 4 (left). The glass beams were placed on timber supports and to support the tempered glass alone, aluminium plates were placed under each tempered glass pane. A steel cage was hung on the beam using two steel rectangles and a steel rod. To add load to the tempered glass alone, aluminium blocks where δ_t had to be larger than the maximum displacement that can occur in the tempered glass, see Fig. 4 (right), were used.

The displacements were measured in both tempered glass panes and the annealed glass, close to the midspan of the beam, using linear potentiometers (POT). Potentiometers were also placed at each end of the annealed glass to monitor the behaviour of the beam at the ends and to see if the loading on the beam was indenting the support.

The shear transfer over time of the interlayers was also investigated by measuring the strains at the top of the annealed glass (compressive zone) and in the steel (tensile zone) close to the midspan of the beam, using strain gauges. The temperature in the room was also monitored. Due to the temperature dependency of the interlayer, temperature was kept relatively high to accelerate the experiments. The temperature was controlled between 27 and 36 °C. No specific time for the duration of the experiment was decided before the experiments were performed. Rather, the experiment was stopped when the desired information about the behaviour of the beam was obtained. The duration of the experiments ranged from 160 to 260 h as shown in Table 1.

3.1 Results

Figure 5 shows the normalized strains in the compression zone of the annealed glass plotted against the duration of the experiment for five of the test specimens. As shown in Fig. 5 there was quite a diversity on the strain development between the tests. High temperature dependency was observed during the experiments which correlates to the properties of the interlayer. When the temperature in the room increased, the interlayer became softer, which resulted in smaller strains due to the increased creep/relaxation of the PVB. As expected, the beams with thicker interlayers had more and faster strain relaxation. Thus, the properties of the interlayer are vital for obtaining the desired behaviour of the glass beam. Soft and thick interlayers will yield faster relaxation of the transferred shear stresses, which will result in lower stresses in the annealed glass. Figure 5 shows that when the load is removed, the strain in the top of the annealed glass changed from compression to tension (vertical lines in the plot). This is due to the tempered glass plies trying to revert back to its original zero-strain position. This could potentially lead to troubles if the applied long-term load is high. Thus, this should

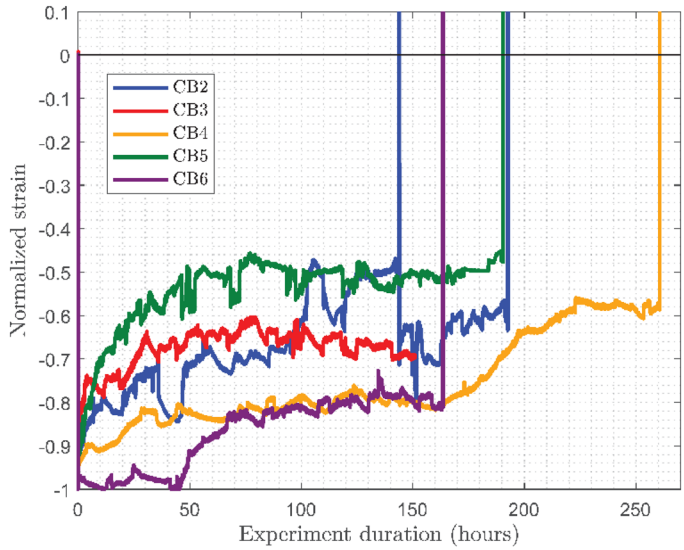

Fig. 5 Normalized strains on the compression zone of the annealed glass versus the duration of the experiment

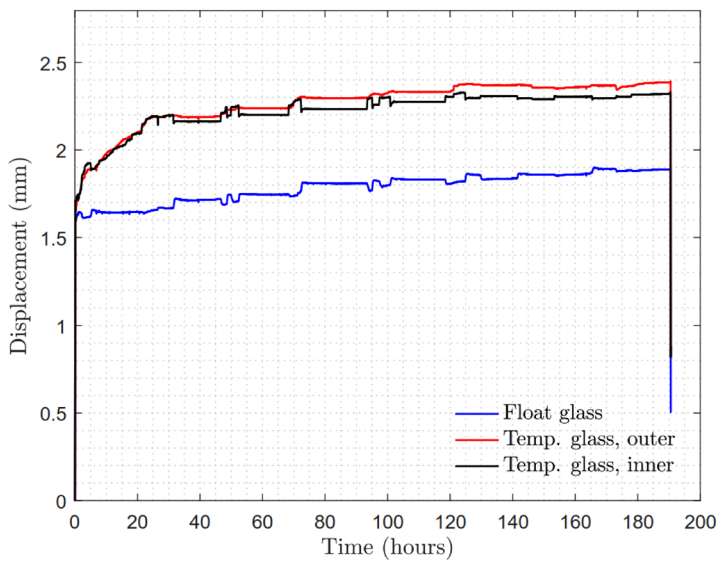

Fig. 6 Displacements (CB5) of the three glass panes over time

be taken into consideration when designing such beams, if high long-term loads are anticipated to be removed quickly at some point in time it could potentially lead to tensile stresses in the annealed glass plies.

The results from the potentiometers at the midspan of the beam showed results that were somewhat expected. Figure 6 shows the displacements of the three glass panes at midspan for the reference specimen.

The displacements at mid-span of the beam showed that the tempered glass panes displaced more than the annealed glass pane, as expected. However, when the strain gauges showed a decrease in strains for the annealed glass, the displacements where still increasing. This is explained by the aluminium plates placed as support conditions, allowing the annealed glass to move rigidly downward. Thus, when the shear stresses in the interlayers were high enough, the ends moved slightly downward to release those stresses (the beam tries to straighten out). The curvature of the beam would thus decrease over time.

Table 2 Parameters for the FE analysis

	Model (a)	Model (b)
E_{glass} (GPa)	70	70
v_{glass} (–)	0.23	0.23
E_{steel} (GPa)	210	210
v_{steel} (–)	0.30	0.30
L_e (mm)	40	50
L_s (mm)	900	900
L_b (mm)	300	–
Load	F = 5692 N	$p = 2 \times 10^6$ N/m^2
Support	Only on tempered glass	Both steel and tempered glass

The columns refer to the load configurations provided in Fig. 7. Interlayer properties are described in Sect. 4.1 and Table 3

4 Finite element study of the concept

For further investigating the concept, a finite element model was established. The modelling was carried out using the commercial FE-software ABAQUS (v. 2019). Since only the response over time in the un-failed state is wanted, both types of glass and the steel is assumed to behave as linear elastic materials (Table 2). The interlayer between the tempered glass and the annealed glass is described by viscoelastic properties as further described in Sect. 4.1. A rigid interface between the steel and the glass is assumed, which is the equivalent of a very thin adhesive layer ($h_a \rightarrow 0$).

Two different load configurations were considered for the beam, (a) four-point bending and (b) uniformly distributed load. Load configuration (a) serves for comparing to experiments while (b) is more relevant for typical engineering purposes.

In order to test the concept at long term loading, the load is applied instantaneously and kept constant over the loading time.

Due to symmetry, only one quarter of the beam is modelled. The elements used were 20 node hexahedral continuum elements (C3D20) and approximately 30 elements were used over the height of the beam as indicated in Fig. 10. Due to the very small variations through the width of the beam, the tempered glass and the interlayer was modelled using one element through the thickness. In order to keep elements with an approximate side ratio of 1:1 three elements were used through the thickness of the annealed glass. The 30 elements used over the height were enough to secure convergence of the results.

4.1 PVB interlayer properties

For the investigated concept, the behaviour of the interlayer is essential and five experimental studies on the PVB interlayer found in the literature was used as the basis for the material parameters used. The relaxation functions for these studies are shown in Fig. 8.

Often designers and engineers do not have relaxation functions for the specific PVB used in a structure. Fitting all the data into an average curve is shown as the solid black line in Fig. 8 which will be assumed to be representative for the PVB interlayers in general. This line is then fitted by a Prony series (solid red line) to provide material data input for the finite element analysis. The Prony series providing the relaxation function, $G(t)$, can be written as:

$$G(t) = \sum_{i=1}^{N} G_i e^{-\frac{t}{\tau_i}} \tag{1}$$

where t is the time and G_i and τ_i is provided in Table 3. The behaviour of the PVB is found by assuming that all relaxation is due to shearing (the bulk modulus, K, will be constant) and a Poisson's ratio of 0.45 is assumed.

Many materials, including PVB, changes viscoelastic properties with temperature which is therefore necessary to account for. The simplest procedure for this is to introduce a temperature dependent time-scale, a so-called shifted time or reduced time. If it is possible to make e.g. relaxation curves for a single material at different temperatures coincide by this it is named a thermorheologically simple material. This has been done in order to generate Table 3 (and Fig. 8) from the references given in the table using the WLF

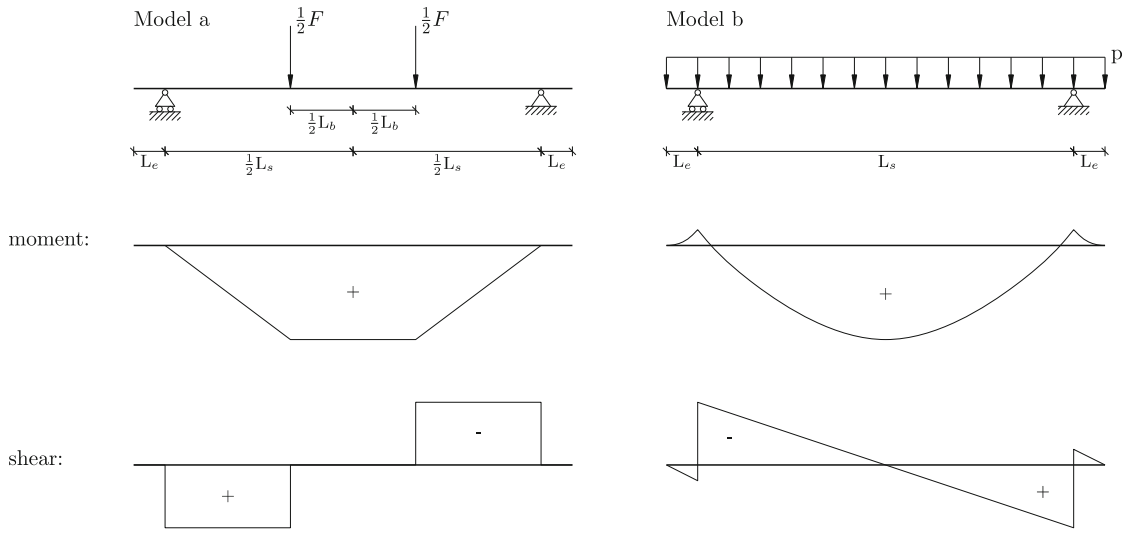

Fig. 7 Static system and cross-sectional force distribution for the load configurations (a) and (b)

(Williams-Landel-Ferry) equation (Williams et al. 1955).

4.2 FE analysis results—model (a)

Model (a), as shown in Fig. 7, considers the same supports and loads as the experiments. Furthermore, the interlayer properties are modelled at 30 °C using the WLF constants given in Table 3(B) in order to represent the experimental conditions. The supports are, in this case, only applied to the tempered glass as was done in the experiments. From this analysis the strain at the top surface (compression) of the annealed glass was -3.16×10^{-4} at t = 0 and -0.83×10^{-4} at t = 200 which is in the same order of magnitude as experimentally found and provided in Table 1.

An increase of ≈ 0.4 mm maximum deflection after the 200 s for the annealed glass was found numerically. In the experiment, approximately 0.3 mm was found (see Fig. 6).

It has to be emphasized that further experimental (and numerical) work needs to be done in order to develop models that can provide accurate results for design, however, the tendencies provided from the numerical models are comparable to the experimental work and are therefore considered useful for investigating the plausibility of the concept.

4.3 FE analysis results—model (b)

For model (b), with a distributed load and both tempered glass and steel supported an analysis to demonstrate some potential of the concept was provided.

The graphs given in Fig. 9 provides the reaction forces (top), stress (middle) and center deflection (bottom) for the beam as a function of time (logarithmic). From the top plot it is seen, as expected, that the total load applied provides a constant total reaction force, however, it is interesting to note that the reaction force from the annealed glass is decreasing over time while the reaction force from the tempered glass takes over. Indicating that the long-term loading is increasingly carried by the tempered glass.

The middle plot shows the first principal stress (where max. moment is present) in the annealed glass and the tempered glass and it is seen that the stress in the annealed glass is decreasing while the principal stress in the tempered glass is increasing. It is also worth noting that the effective stress in the steel is decreasing as well. Since the major part of the stress in the steel is longitudinal it must be interpreted as the normal force in the steel is decreasing as well. This indicates that the needed shear transfer in the adhesive between the steel and the annealed glass is also decreasing to the benefit for the lifetime of such beam. The bottom plot shows that while the tempered glass

increases its deflection (approaching a limit) the annealed glass decreases its deflection over time.

In Fig. 10 the cross sectional displacements for model (b) is shown. It is seen that the behaviour is as expected where the tempered glass takes and increasing part of the load and the annealed glass moves towards zero load conditions. From this figure (and the previous), it is also seen that the annealed glass is never reaching a maximum principal stress of more than 26 MPa. Utilising a higher short-term strength of the annealed glass would provide a more efficient design.

5 Discussion

For the results presented in Fig. 9 a reduction from 26 MPa (at t = 1 s) to 11 MPa (at t = 10 yr) is seen. Considering a traditional reinforced glass beam consisting of annealed glass, the stresses would not be redistributed. In this case the stress would be 26 MPa during all 10 years. Using the following theory (Beason and Morgan 1984) we can calculate an equivalent stress, σ_{eq}, that can be compared to the 26 MPa.

$$\sigma_{eq} = \left[\frac{1}{t_f} \int_{t=0}^{t=t_f} \sigma(t)^n dt \right]^{\frac{1}{n}}, \quad \text{where} \quad n = 16 \text{ is a typical value for annealed glass} \tag{2}$$

To simplify the calculations we approximate the stress over time as plotted in Fig. 9 with a straight line in a semi logarithmic plot in the interval $t \in [1\,\text{s}; 10\,\text{year}]$ and furthermore assume a constant stress during the first second of loading. The stress as a function of time becomes:

$$\sigma(t) = \begin{cases} 26 & \text{for} \quad 0 < t < 1\,\text{s} \\ 26 - 0.767 \cdot \log_e(t) & \text{for} \quad t > 1\,\text{s} \end{cases} \tag{3}$$

Inserting (3) in (2), using $n = 16$ and performing the integration for changing values of t_f, the following plot is obtained.

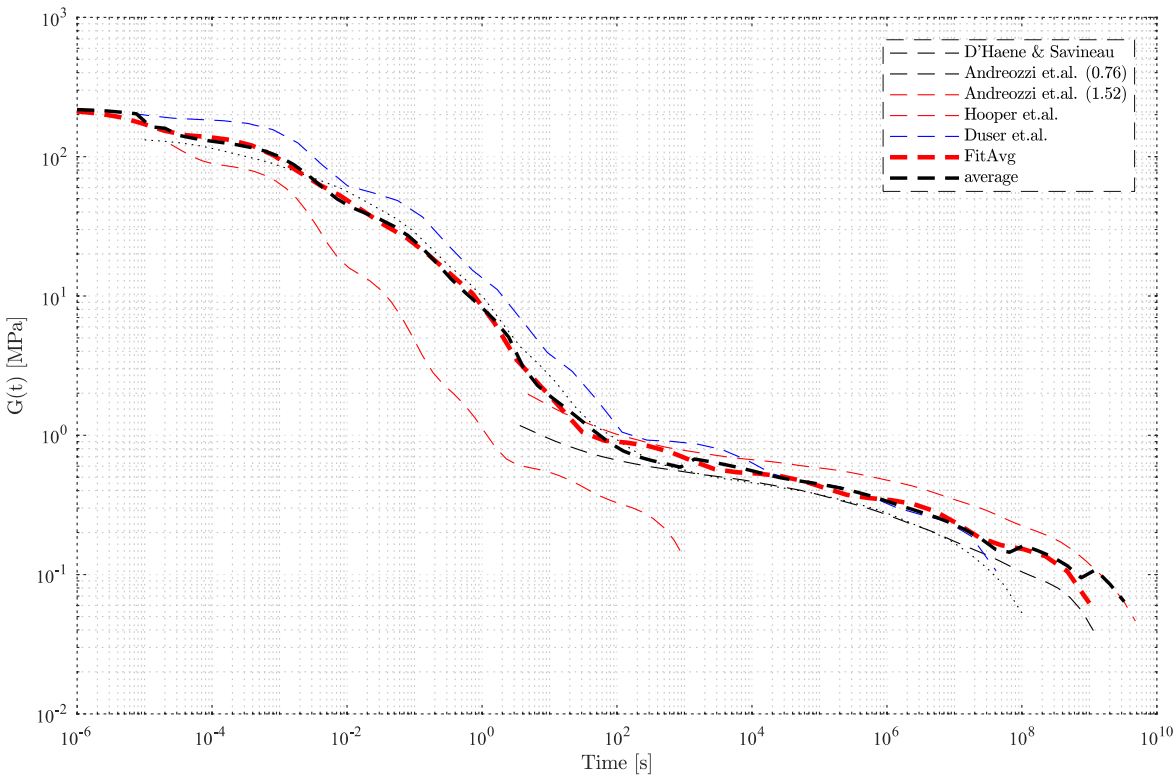

Fig. 8 PVB relaxation functions from different authors

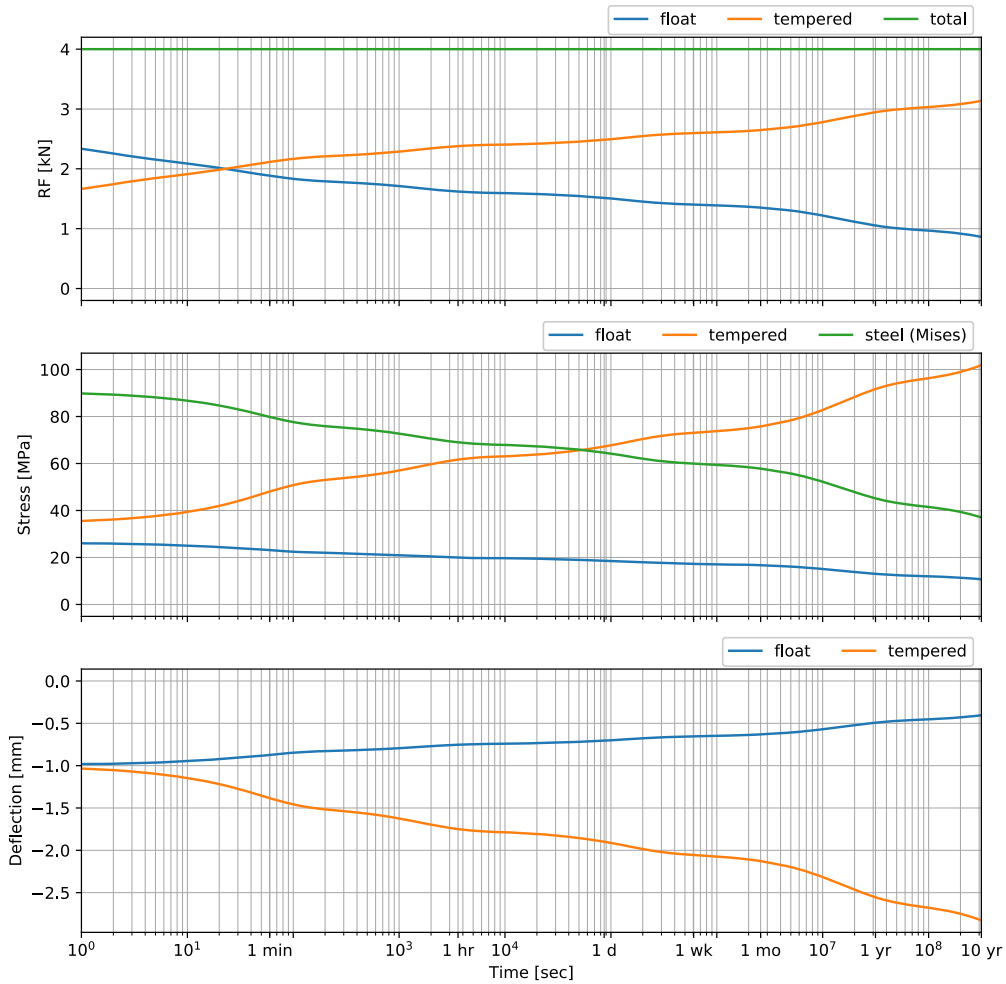

Fig. 9 Results from the FE analysis. Top: reaction forces, Middle: stresses, Bottom: deflection. Note that the curves start when all the (constant) load is applied

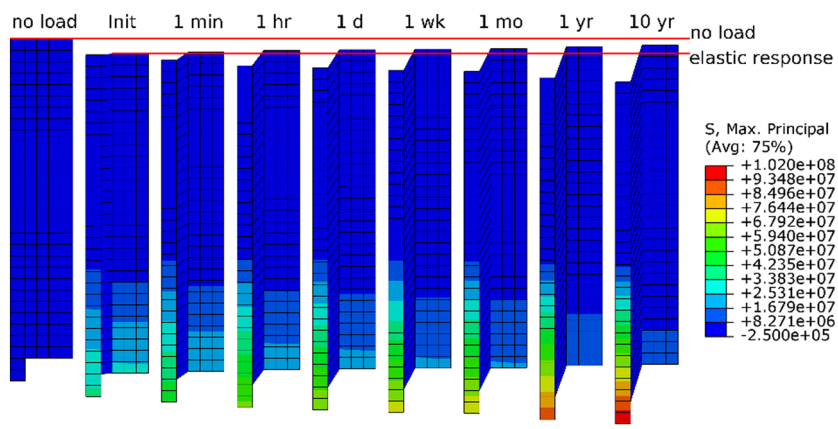

Fig. 10 Cross-sectional displacements and max principal stress (in Pa). Note that only one-half of the model is shown (tempered/PVB/annealed) and deformations are scaled by a factor of 4. The "init" cross section is the short-term response to the load

Table 3 Parameters for the Prony series at T = 20 °C from different authors

(A) (Andreozzi et al. 2014)		(B) (Andreozzi et al. 2014)		(C) (D'Haene and Savineau 2007)		(D) (Hooper et al. 2012)		(E) (Duser et al. 1999)		(F) Fit average	
$c_1 = 12.5, c_2 = 89$		$c_1 = 12.1, c_2 = 82$		Provided at 20 °C		–		Provided at 20 °C		Provided at 20 °C	
$\sum G_i$ = 1.56 MPa		$\sum G_i$ = 2.74 MPa		$\sum G_i$ = 136.12 MPa		$\sum G_i$ = 178.23 MPa		$\sum G_i$ = 471.11 MPa		$\sum G_i$ = 377.20 MPa	
G_i	τ_i	G_i	τ_i	G_i	τ_i	G_i	τ_i	G_i	τ_i	G_i	τ_i
0.5146	3.63E+00	1.0663	4.79E+00	2.268	1E−05	87.2485	2.45E−05	7.56E+01	3.26E−11	1.59E+02	1.00E−07
0.2801	1.80E+01	0.5604	2.82E+01	25.233	1E−04	72.7023	2.21E−03	3.71E+01	4.95E−09	7.37E+01	1.00E−05
0.1443	1.04E+02	0.2795	2.07E+02	30.845	1E−03	15.1692	4.98E−02	1.37E+02	7.24E−08	7.05E+01	1.00E−03
0.0869	8.06E+02	0.1352	1.92E+03	29.222	1E−02	2.4724	6.24E−01	3.35E+01	9.86E−06	3.63E+01	1.00E−02
0.0762	8.45E+03	0.087	2.54E+04	29.188	1E−01	0.283	2.49E+01	1.27E+02	2.81E−03	1.98E+01	1.00E−01
0.0922	8.10E+04	0.1048	3.47E+05	14.231	1E+00	0.356	1.00E+03	4.22E+01	1.64E−01	1.42E+01	1.00E+00
0.0988	6.65E+05	0.1342	3.62E+06	3.718	1E+01			1.42E+01	2.26E+00	2.76E+00	1.00E+01
0.0856	5.01E+06	0.1354	3.54E+07	0.743	1E+02			3.58E+00	3.54E+01	3.83E−01	1.00E+03
0.0703	4.01E+07	0.1111	5.27E+08	0.167	1E+03			4.54E−01	9.37E+03	1.89E−01	1.00E+05
0.1077	1.14E+09	0.126	4.79E+09	0.071	1E+04			1.91E−01	6.41E+05	1.95E−01	1.00E+07
				0.081	1E+05			2.89E−01	4.13E+07	1.69E−01	1.00E+09
				0.11	1E+06						
				0.103	1E+07						
				0.144	1E+08						
G_{10} = 0.94 MPa		G_{10} = 1.62 MPa		G_{10} = 2.72 MPa		G_{10} = 0.52 MPa		G_{10} = 3.81 MPa		G_{10} = 1.95 MPa	

Parameters in (A) and (B) have shifted from T = 30 °C to T = 20 °C in the table using the WLF equation and associated parameters. (A) and (B) are reported from tests on PVB thicknesses. $\sum G_i$ is the instantaneous shear moduli and G_{10} is the moduli after 10 s for the different relaxation functions

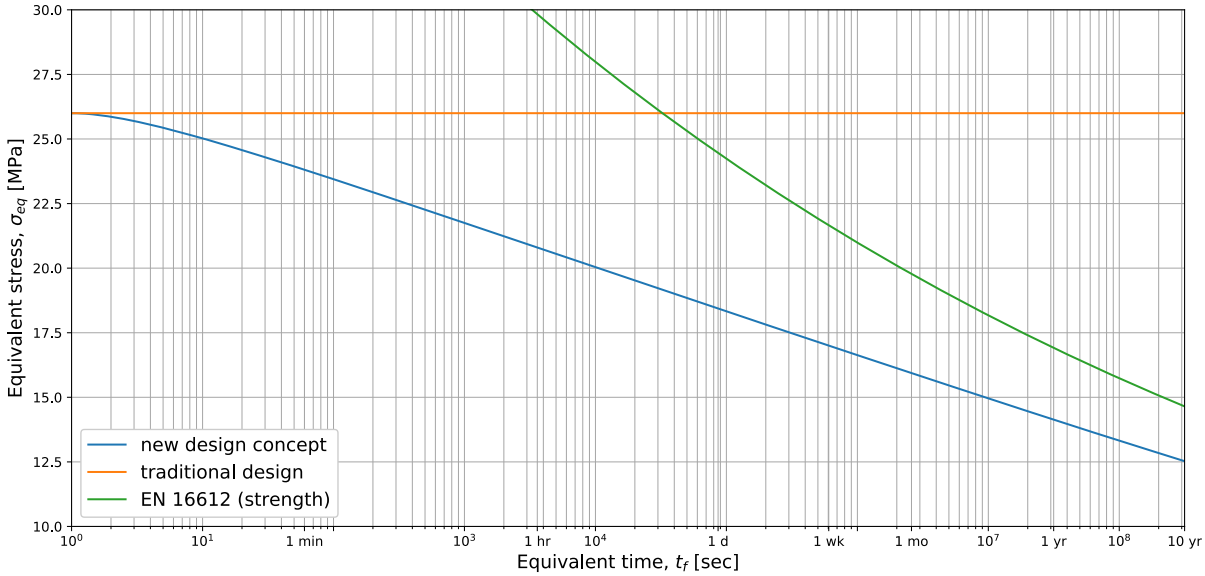

Fig. 11 Evolution of equivalent stress. Equivalent constant stress applied in a given time, t_f. Green line represents the time-dependent strength of annealed glass

The characteristic time dependent strength,[1] f_{time}, of annealed glass accoding to EN 16612:2019 can be calculated as:

$$f_{time} = f_0 \cdot 0.663 \cdot t^{-\frac{1}{16}} \tag{4}$$

where t is the time in hours, $f_0 = 45$ MPa is used as the characteristic short term strength of annealed glass for producing the curve in Fig. 11.

In a traditional design, the annealed glass is not capable of redistributing the stresses from the long term loading and the beam has to carry the designed long-term load (in this case 26 MPa). The new concept redistributes the long-term loading and for a permanent load of e.g. 26 MPa (initially) it is seen from Fig. 11, that the stress in the annealed glass (for the new concept) is below the characteristic glass strength according to EN 16612. Furthermore, it is seen that the lifetime (until first crack) of the traditional design would, with the applied load, be less than one day.

6 Conclusion

Although the suggested concept needs further investigation, the potential seems evident from the investigations carried out in the present paper. The experimental work clearly demonstrates the tendencies for transferring long-term stresses from the annealed glass to the tempered glass as the compressive strains are lowered over time. The same was observed for the deflections of the tempered glass, which increased over time, as expected for the concept.

The numerical model showed a reduction from 26 MPa to approximately 20 MPa after 1 h and further down to 13 MPa after 1 year and 11 MPa after 10 years. This reduction results in a considerable decrease in damage (due to static fatigue) in the annealed glass. The reduction of stress over time is increasing the life-time of the beam and in the presented case, the stress stays below the time-dependent strength of the annealed glass. It should be emphasized here that the calculations provided in this paper were not optimised with respect to material usage. An optimization parameter would be to allow the annealed glass an initial stress of its short-term tensile strength.

Compliance with ethical standards

Conflict of interest On behalf of all authors, the corresponding author states that there is no conflict of interest.

[1] Only the time-dependency (k_{mod}) from the expression in EN 16612:2019 is considered here.

References

Andreozzi, L., Briccoli Bati, S., Fagone, M., Ranocchiai, G., Zulli, F.: Dynamic torsion tests to characterize the thermo-viscoelastic properties of polymeric interlayers for laminated glass. Constr. Build. Mater. **65**, 1–13 (2014). https://doi.org/10.1016/j.conbuildmat.2014.04.003

Beason, W.L.W., Morgan, J.R.: Glass failure prediction model. J. Struct. Eng. **110**, 197–212 (1984). https://doi.org/10.1061/(ASCE)0733-9445(1985)111:9(2058)

Bedon, C., Louter, C.: Finite-element analysis of post-tensioned SG-laminated glass beams with mechanically anchored tendons. Glass Struct. Eng. **1**, 39–59 (2016). https://doi.org/10.1007/s40940-016-0020-7

Ber, B., Premrov, M., Štrukelj, A.: Finite element analysis of timber-glass walls. Glass Struct. Eng. **1**, 19–37 (2016). https://doi.org/10.1007/s40940-016-0015-4

Bos, F.P., Veer, F., Hobbelman, G.J., Louter, C.: Stainless steel reinforced and post-tensioned glass beams. In: 12th International Conference on Experimental Mechanics, pp. 1–9 (2004)

Brown, W.G. (1969) A load duration theory for glass design. In: Proceedings Annual Meeting of the international Commision on Glass. Toronto (1969)

Charles, R.J.: Static fatigue of glass. II. J. Appl. Phys. **29**, 1554–1560 (1958a). https://doi.org/10.1063/1.1722992

Charles, R.J.: Dynamic fatigue of glass. J. Appl. Phys. **29**, 1657–1662 (1958b). https://doi.org/10.1063/1.1723019

Cupać, J., Martens, K., Nussbaumer, A., Belis, J., Louter, C.: Experimental investigation of multi-span post-tensioned glass beams. Glass Struct. Eng. **2**, 3–15 (2017). https://doi.org/10.1007/s40940-017-0038-5

D'Haene, P., Savineau, G. (2007) Mechanical properties of laminated safety glass—FEM study. In: Glass Processing Days, Tampere, Finland (2007)

EN 16612:2019: Determination of the lateral load resistance of glass panes by calculation. (2019)

Feldmann, M., Di Biase, P.: The CEN-TS "structural glass - design and construction rules" as pre-standard for the Eurocode. ce/papers. **2**, 71–80 (2018). https://doi.org/10.1002/cepa.911

Freytag, B.: Glass-concrete composite technology. Struct. Eng. Int. **14**, 111–117 (2004)

Hooper, P.A., Blackman, B.R.K., Dear, J.P.: The mechanical behaviour of poly(vinyl butyral) at different strain magnitudes and strain rates. J. Mater. Sci. **47**, 3564–3576 (2012). https://doi.org/10.1007/s10853-011-6202-4

Louter, C.L.P.C.: Fragile yet Ductile: Structural Aspects of Reinforced Glass Beams, Ph.D. Thesis, TU Delft (2011)

Louter, C., Belis, J., Veer, F., Lebet, J.-P.: Structural response of SG-laminated reinforced glass beams; experimental investigations on the effects of glass type, reinforcement percentage and beam size. Eng. Struct. **36**, 292–301 (2012). https://doi.org/10.1016/j.engstruct.2011.12.016

Martens, K., Caspeele, R., Belis, J.: Numerical investigation of two-sided reinforced laminated glass beams in statically indeterminate systems. Glass Struct. Eng. **1**, 417–431 (2016a). https://doi.org/10.1007/s40940-016-0005-6

Martens, K., Caspeele, R., Belis, J.: Load-carrying behaviour of interrupted statically indeterminate reinforced laminated glass beams. Glass Struct. Eng. **1**, 81–94 (2016b). https://doi.org/10.1007/s40940-016-0017-2

Martens, K., Caspeele, R., Belis, J.: Experimental investigation into the effects of membrane action for continuous reinforced glass beam systems. Glass Struct. Eng. **3**, 389–402 (2018). https://doi.org/10.1007/s40940-018-0076-7

Møller, R.N., Andersen, A.L.: Analysis of Mechanically Reinforced Glass Beams, MSc Thesis, Technical University Denmark, in danish (2010)

Nielsen, J.H.: Remaining stress-state and strain-energy in tempered glass fragments. Glass Struct. Eng. **2**, 45–56 (2017). https://doi.org/10.1007/s40940-016-0036-z

Nielsen, J.H., Bjarrum, M.: Deformations and strain energy in fragments of tempered glass: experimental and numerical investigation. Glass Struct. Eng. (2017). https://doi.org/10.1007/s40940-017-0043-8

Nielsen, J.H., Olesen, J.F.: Mechanically reinforced glass beams. In: Recent Developments in Structural Engineering, Mechanics and Computation, pp. 1707–1712. Cape Town, South Africa (2007)

Nielsen, J.H., Olesen, J.F.: Post-crack capacity of mechanically reinforced glass beams (MRGB). In: Oh, B.H., et al. (eds.) Fracture Mechanics of Concrete and Concrete Structures, 7, pp. 370–376. RILEM, Jeju (2010)

Nielsen, J.H., Olesen, J.F., Stang, H.: The fracture process of tempered soda-lime-silica glass. Exp. Mech. **49**, 855–870 (2009). https://doi.org/10.1007/s11340-008-9200-y

Ølgaard, A.B., Nielsen, J.H., Olesen, J.F.: Design of mechanically reinforced glass beams: modelling and experiments. Struct. Eng. Int. **19**, 130–136 (2009). https://doi.org/10.2749/101686609788220169

Pour-Moghaddam, N.: On the fracture behaviour and the fracture pattern morphology of tempered soda-lime glass. Springer Fachmedien Wiesbaden, Wiesbaden (2020)

Vallee, T., Grunwald, C., Milchert, L., Fecht, S.: Design and dimensioning of a complex timber-glass hybrid structure: the IFAM pedestrian bridge. Glass Struct. Eng. **1**, 3–18 (2016). https://doi.org/10.1007/s40940-016-0007-4

Van Duser, A., Jagota, A., Bennison, S.J.: Analysis of glass/polyvinyl butyral laminates subjected to uniform pressure. J. Eng. Mech. **125**, 435–442 (1999). https://doi.org/10.1061/(ASCE)0733-9399(1999)125:4(435)

Veer, F.A., Rijgersberg, H., Ruytenbeek, D., Louter, P.C., Zuidema, J.: Composite Glass Beams, the Third Chapter. In: Glass Processing Days 2003, pp. 307–310. Tampere, Finland (2003)

Wellershoff, F., Sedlacek, G.: Structural use of glass in hybrid elements: steel-glass-beams, glass-GFRP-plates. In: Proceedings of Glass Processing Days 2003, pp. 268–270 (2003)

Williams, M.L., Landel, R.F., Ferry, J.D.: The temperature dependence of relaxation mechanisms in amorphous polymers and other glass-forming liquids. J. Am. Chem. Soc. **77**, 3701–3707 (1955). https://doi.org/10.1021/ja01619a008